Recovery of central memory and naive peripheral t cells in follicular Lymphoma patients receiving rituximab-chemotherapy based regimen

B Milcent, N. Josseaume, F. Petitprez, Q. Riller, S Amorim, P. Loiseau, A. Toubert, P. Brice, C. Thieblemont, J.-L Teillaud, et al.

SCIENTIFIC REPORTS
nature research

OPEN

Recovery of central memory and naive peripheral T cells in Follicular Lymphoma patients receiving rituximab-chemotherapy based regimen

Received: 21 May 2019
Accepted: 4 September 2019
Published online: 17 September 2019

B. Milcent[1,2,3], N. Josseaume[1,2,3], F. Petitprez[1,2,3,4], Q. Riller[1,2,3], S. Amorim[5], P. Loiseau[6,7,8], A. Toubert[6,7,8], P. Brice[5], C. Thieblemont[5,9], J.-L. Teillaud[1,2,3,10] & S. Sibéril[1,2,3]

Preclinical models and clinical studies have shown that anti-CD20-based treatment has multifaceted consequences on T-cell immunity. We have performed a prospective study of peripheral T-cell compartment in FL patients, all exhibiting high tumor burden and receiving rituximab-chemotherapy-based regimen (R-CHOP). Before treatment, FL patients harbor low amounts of peripheral naive T cells, but high levels of $CD4^+$ T_{EM}, $CD4^+$ T_{reg} and $CD8^+$ T_{EMRA} subsets and significant amounts of $CD38^+$ $HLA\text{-}DR^+$ activated T cells. A portion of these activated/differentiated T cells also expressed PD-1 and/or TIGIT immune checkpoints. Hierarchical clustering of phenotyping data revealed that 5/8 patients with only a partial response to R-CHOP induction therapy or with disease progression segregate into a group exhibiting a highly activated/differentiated T cell profile and a markedly low proportion of naive T cells before treatment. Rituximab-based therapy induced a shift of $CD4^+$ and $CD8^+$ T cells toward a central memory phenotype and of $CD8^+$ T cells to a naive phenotype. In parallel, a decrease in the number of peripheral T cells expressing both PD-1 and TIGIT was detected. These observations suggest that the standard rituximab-based therapy partially reverts the profound alterations observed in T-cell subsets in FL patients, and that blood T-cell phenotyping could provide a better understanding of the mechanisms of rituximab-based treatment.

Follicular lymphoma (FL) is the second most common form of non-Hodgkin lymphoma (NHL). Its clinical course is highly variable and survival medians are 7–15 years depending on the studies. Follicular lymphoma management is characterized by a risk-adapted therapy based on the stage of the disease and the symptoms of the patients. For high tumor burden patients, treatment options could be either rituximab plus cyclophosphamide, vincristine and prednisone with (R-CHOP) or without (R-CVP) doxorubicin or other anthracyclines, or rituximab plus fludarabine for patients not eligible for anthracyclines, or rituximab plus bendamustine. Experimental therapies as well as allogeneic stem cell transplantation are rather considered for relapsed and more refractory disease[1]. The addition of the anti-CD20 monoclonal antibody (mAb) rituximab to chemotherapy has resulted in a higher rate of complete remission and improved survival[2]. In addition, rituximab as maintenance therapy

[1]Cordeliers Research Center-Inserm UMR-S 1138, "Cancer, Immune Control and Escape" Laboratory, Paris, 75006, France. [2]Sorbonne Université, UMR-S 1138, Paris, 75006, France. [3]Paris Descartes-Paris 5 University, UMR-S 1138, Paris, 75006, France. [4]Ligue Nationale Contre le Cancer, Programme Cartes d'Identité des Tumeurs, Paris, 75014, France. [5]APHP, Saint-Louis Hospital, Hemato-oncology – Diderot University, Sorbonne Paris Cité, Paris, France. [6]Laboratoire d'Immunologie et Histocompatibilité, Hôpital Saint-Louis, Paris, France. [7]Inserm UMR-S 1160, Paris, France. [8]Institut Universitaire d'Hématologie, Université Paris Diderot, Paris, 7, France. [9]EA7324 Université Paris Descartes, Sorbonne Paris Cité, Paris, France. [10]Present address: Laboratory "Immune Microenvironment and Biotherapy", Sorbonne University UMRS1135, INSERM U.1135, Centre d'Immunologie et des Maladies Infectieuses (CIMI), Paris, France. B. Milcent and N. Josseaume contributed equally. J.-L. Teillaud and S. Sibéril jointly supervised this work. Correspondence and requests for materials should be addressed to S.S. (email: sophie.siberil@sorbonne-universite.fr)

after induction regimen improves progression-free survival (PFS) in high-tumor burden patients[3]. Nonetheless, about 15–20% of patients fail to respond to chemo-immunotherapy and die prematurely. New clinical-genetic predictors have been recently proposed to identify subgroups of patients at high risk of early failure of first-line immune-chemotherapy and disease progression (m7-FLIPI and POD24-PI)[4,5]. Huet *et al*. have also recently developed and validated a gene-expression profiling score applicable to formalin-fixed, paraffin-embedded tumor biopsies from patients with follicular lymphoma for predicting clinical outcome[6]. The gene signature defined in this study is characteristic of B-cell biology and tumor microenvironment. Gene expression profiling and molecular studies, as well as multiple immunochemistry and flow cytometry analyses of the microenvironment in lymph node biopsies have also highlighted the role of non-malignant immune cells and in particular tumor-infiltrating T cells (TIL) on outcomes of FL patients[7–19]. Only a few studies, however, have analyzed the relations between patient peripheral T-cell subsets and their clinical outcome[15,20–23]. The different therapies that have been used in cohorts of FL patients have complicated our understanding of the role of host adaptive immunity as many of them impacted both tumor and normal immune cells[24,25]. The infusion of anti-CD20 mAb affects T-cell compartments, as shown in both preclinical models and patients with inflammatory/autoimmune diseases or tumors[26,27]. Moreover, studies of mice engrafted with $CD20^+$ tumor cells have demonstrated that anti-CD20 treatment, in addition to its antitumor effect based on innate immunity, has a major effect on tumor immune-surveillance through the development of long-term antitumor T-cell immunity[28–31]. Notably, we have previously shown that anti-CD20 treatment modifies the phenotype of $CD4^+$ T cells by preventing the expansion of protumor $CD4^+$ T_{reg} cells and inducing polarization towards a Th1 phenotype through the IFN-γ/IL-12 axis[29]. Anti-CD20-based treatment can have therefore multifaceted consequences on host adaptive immunity and affect T-cell subsets. An integrated phenotypic profiling of peripheral T-cell subsets in patients with follicular lymphoma before and during treatment could therefore provide a better understanding of the mechanisms of rituximab-based treatment.

We analyzed here the peripheral T-cell subset distribution in 33 FL patients with high tumor burden before any treatment. Thus, consistently with the PRIMA phase III study[3], all patients received six cycles every 21 days of R-CHOP induction therapy. R-CHOP responder patients then received rituximab maintenance for two years. We report here a bias in peripheral T-cell subset distribution in 33 FL patients with high tumor burden before any treatment. Hierarchical clustering of multiparametric flow cytometry data revealed a group of patients characterized by a high proportion of both activated and PD-1/TIGIT expressing T cells. A significantly higher number of patients with partial response to rituximab-based therapy and with disease progression was observed in this group. These patients exhibited lower percentages of naive $CD4^+$ T cells as compared to others FL patients. Moreover, the standard rituximab-based therapy in FL patients with high tumor burden induced the skewing of the effector memory phenotype towards a central memory and naive T-cell phenotype.

Results

Peripheral T-cell subsets in untreated FL patients differ from those in healthy donors. 33 high-tumor burden FL patients (grade I-III), with a majority of them (>80%) being in advanced stages III-IV of the disease, were enrolled in a prospective phenotypic study (Table 1). All patients were homogenously treated with an induction therapy containing rituximab and chemotherapy (R-CHOP) followed by either rituximab maintenance or chemotherapy-based consolidation regimens (Fig. 1 and Supplementary Table S1).

We first examined T-cell blood compartments of FL patients before any treatment. The percentages of $CD4^+$ and $CD8^+$ T cells did not differ between patients before treatment (FL-T0) and healthy donors (HD) (data not shown). However, when T-cell subsets were analyzed in detail, we observed that FL-T0 patients had a lower percentage of naive $CD4^+$ T_N and $CD8^+$ T cells than healthy donors did (Fig. 2a,b). Inversely, the percentages of $CD4^+$ T_{EM}, $CD4^+$ T_{reg} (defined as $CD25^+CD127^-$) and of $CD8^+$ T_{EMRA} were higher (Fig. 2a,b). Of note, the percentage of $CD4^+$ T_{EMRA} was very low (<1%) (data not shown). Thus, subsets among this latter population were not further analyzed.

The activation status of blood T cells before any treatment was also compared to that of healthy donors (Fig. 2). The percentages of $CD4^+$ and $CD8^+$ T cells expressing CD38 and HLA-DR were significantly increased (Fig. 2c, left panels) due to an increase in the percentages of $CD38^+$HLA-DR^+ T_{EM}, T_{CM}, and T_{EMRA} cells (Supplementary Fig. S1). Moreover, the percentages of peripheral $CD4^+$ and $CD8^+$ T cells expressing PD-1 and TIGIT immune checkpoint molecules (ICP) were high (Fig. 2c middle and right panels), with up to 40–60% of T cells in some patients expressing these ICP. In contrast, the percentage of peripheral T cells expressing OX40, CD40L, GITR, 4-1BB, LAG3 and TIM3 was low, with a median value of stained cells below 1% in most cases (Supplementary Fig. S2). Higher percentages of $CD45RA^-$ T_{reg} and $CD26^-$ $CD39^+$ T_{reg}, as well as of PD-1^+ or $PD1^+$CTLA-4^+ T_{reg}, were also observed in FL patients suggesting an activation of this T-cell subset with an immunosuppressive capacity (Fig. 2d).

We then used an antibody panel (panel 4; Supplementary Table S2) to compare the expression and co-expression of CD38, HLA-DR, PD-1, and TIGIT in different T-cell subsets (Fig. 3). In line with the data reported above, T_{CM}, T_{EM}, and T_{reg} rather than naive T cells expressed CD38 and HLA-DR activation markers (Fig. 3a). Similarly, higher percentages of T_{CM} and T_{EM} expressed PD-1, TIGIT, or both molecules as compared to naive T cells (Fig. 3b). In addition, a large number of $CD8^+$ T_{EMRA} cells expressed TIGIT (Fig. 3b, middle panel) and a high proportion of T_{reg} was PD-1^+ (Fig. 3b, left panel). Moreover, the frequency of $CD4^+$/$CD8^+$ T cells expressing CD38 and/or HLA-DR among $CD4^+$/$CD8^+$ PD-1^+TIGIT$^+$ T cells was significantly higher than among $CD4^+$/$CD8^+$ PD-1^-TIGIT$^-$ T-cell subset ($p = 0.0006$ for both $CD4^+$ and $CD8^+$ T cells, using unpaired *t* tests) (Fig. 3c,d).

These data highlighted the presence in the blood of untreated FL patients of a substantial amount of $CD4^+$ or $CD8^+$ activated T cells also expressing PD-1 and TIGIT ICP. Of note, *in vitro* IFN-γ responses of PBMC from patients against CEFT peptides, derived from viruses commonly infecting large numbers of individuals (CMV,

Age at initiation of treatment (median ± S.D.) ($n = 33$)*	59 ± 10.77
Sex ($n = 33$)	
Female	14/33 (42%)
Male	19/33 (58%)
Grade ($n = 33$)	
Grade I-II	30/33 (90.9%)
Grade III	3/33 (9.1%)
Ann Arbor stage ($n = 33$)	
I	1/33 (3.1%)
II	4/33 (12.1%)
III	11/33 (33.3%)
IV	17/33 (51.5%)
LDH elevated ($n = 33$)	7/33 (21.2%)
Serum Beta-2 microglobuline elevated ($n = 15$)	11/15 (73.3%)
Hemoglobin ≥ 12 g/dL ($n = 33$)	31/33 (94%)
Longer diameter of the largest involved node > 6 cm ($n = 24$)	13/24 (54.2%)
FLIPI score[a] ($n = 33$)	
FLIPI ≤ 1	8/33 (24.2%)
FLIPI = 2	16/33 (48.5%)
FLIPI ≥ 3	9/33 (27.3%)

Table 1. Patients clinical characteristics before treatment. *n = Total number of patients for which the clinical data were available. [a]Follicular Lymphoma International Prognostic Index (FLIPI) is based on a combined score of five parameters that include age (>60 *vs* ≤60 years), stage (III-IV *vs* I-II), anemia (hemoglobin <12 *vs* ≥12 dg/L), number of involved node areas (>4 *vs* ≤4) and serum LDH (elevated *vs* normal). FLIPI scores ≤1, 2, ≥3 classify patients into three groups with 10-year overall OS rates of 71%, 51% and 36%, respectively[51].

EBV, influenza) or from tetanus toxin, were similar to responses obtained with healthy donors (Supplementary Fig. S3).

Taken together, the decreased percentage of naive T cells associated with higher percentages of differentiated cells *(i.e.*, T_{EM}, T_{CM}, T_{EMRA} and T_{reg} cells) expressing both activation markers and ICP molecules likely reflect an activation of T cells accompanying tumor development in FL patients prior to any treatment.

High level of differentiated T cells expressing activation markers and PD-1/TIGIT ICP is related to the disease. Changes in peripheral T-cell compartments may be age-related as previously reported for naive and T_{EMRA} $CD8^+$ T cells in other studies[32,33]. Thus, we performed correlation analysis between age and flow cytometry data in FL patients before treatment. The percentages of $CD4^+$ and $CD8^+$ T_N, $CD4^+$ T_{EM}, $CD8^+$ T_{EMRA}, and of $CD4^+CD38^+HLA\text{-}DR^+$ cells correlated with age (Supplementary Fig. S4). In contrast, age had no influence on the percentages of T_{reg} or of $PD\text{-}1^+$ and $TIGIT^+$ T cells. Also, no correlation was found between age and the percentage of $CD4^+$ and $CD8^+$ differentiated T cells (T_{EM}, T_{CM}, T_{EMRA}) expressing both CD38 and HLA-DR (Supplementary Fig. S4). These results indicate that a part of peripheral T-cell phenotype alterations observed in untreated high-tumor burden patients is not related to age but to the disease.

Patients with partial responses to R-CHOP or with early progression of the disease exhibit low percentages of naive $CD4^+$ T cells before treatment. An unsupervised hierarchical clustering based on flow cytometry values obtained from the 33 patients was performed. We selected the data obtained with antibody panels #1, #2 and #3 (Supplementary Table S2) but not all the combinations from each panel were used. We excluded values ($CD4^+$ T_{EMRA}, OX40, CD40L, GITR, 4-1BB, LAG3 and TIM3 $CD4^+$ or $CD8^+$ T cells) for which the patients exhibited very low percentages (median value of stained cells below 1% in most cases). Three other values (% $CD26^+CD39^-/T_{reg}$, % $CD26^+CD39^+/T_{reg}$, % $CD26^-CD39^+/T_{reg}$) for which we have the data from only 19 patients were also excluded. It demonstrated that, before treatment (FL-T0), a marked heterogeneity of the phenotypic profiles can be observed between patients (Fig. 4a). Three groups of patients with particular blood T-cell profiles could be identified. Group 1 ($n = 16$) is characterized by a low-level activation profile with a high frequency of naive $CD38^-HLA\text{-}DR^-$ $CD4^+$ and $CD8^+$ T cells and low proportions of $CD4^+$ T cells expressing TIGIT. Moreover, in this group of patients, T_{EM}, T_{CM} and T_{EMRA} subsets are mainly $CD38^-HLA\text{-}DR^-$. Inversely, patients from group 3 ($n = 9$) exhibited a high frequency of T_{CM}, T_{EM}, T_{EMRA} subsets expressing CD38 and/or HLA-DR activation markers. Patients of group 3 also exhibited high percentages of $PD1^+$ and $TIGIT^+$ $CD4^+$ T cells. Finally, group 2 ($n = 8$) is characterized by intermediate activation profiles with high percentages of $CD38^-HLA\text{-}DR^-$ or $CD38^+HLA\text{-}DR^-$ T_{CM}, T_{EM} and T_{EMRA} subsets and low percentages of T cells expressing PD-1 and TIGIT (Fig. 4a).

Among the 33 patients included in this study, 6 patients exhibited a partial response (PR) to the induction treatment (6 cycles of R-CHOP) and received a consolidation therapy based on chemotherapy combined to rituximab infusion. Tumor progression occurred later on for three of them. Moreover, 2/33 patients exhibited a disease progression during maintenance treatment (rituximab as a single agent) (Fig. 1 and Supplementary Table S1).

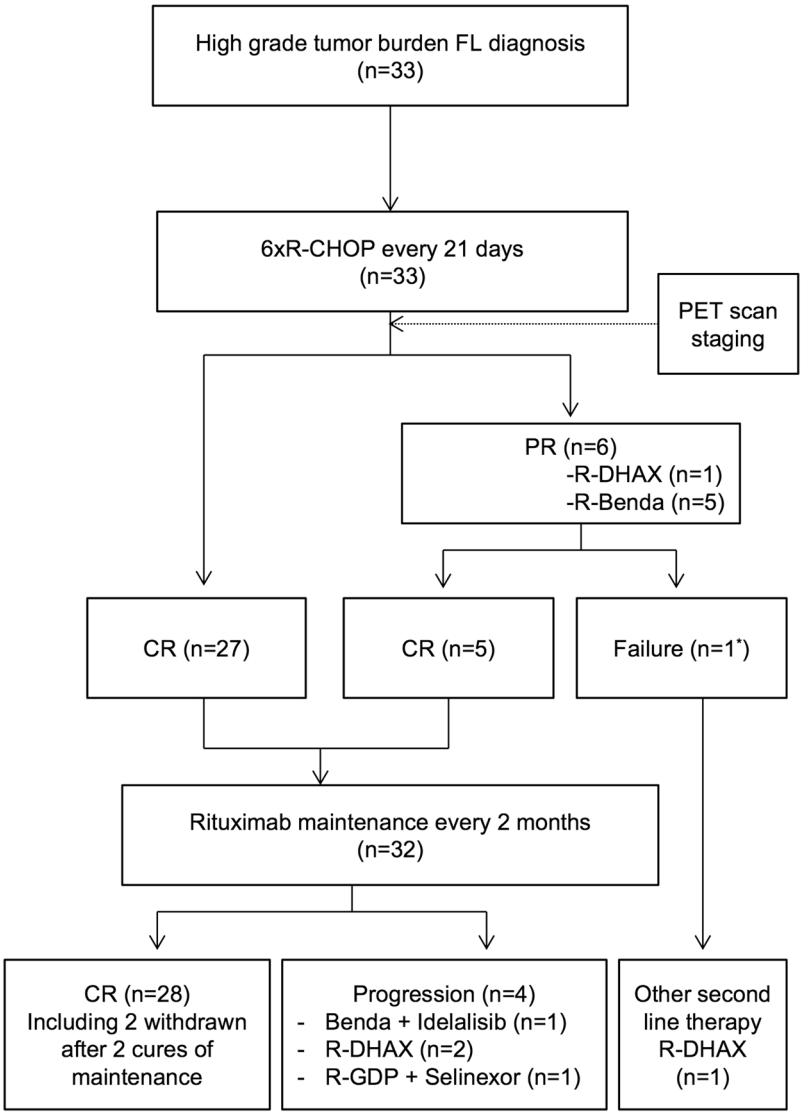

Figure 1. Flowchart of patients included in the study. The study included 33 patients diagnosed with high-tumor-burden Follicular Lymphoma (FL). The patients were treated with regimens based on rituximab and chemotherapy. CR = Complete Response. PR = Partial Response. PET = Positron Emission Tomography. R = rituximab. CHOP = cyclophosphamide, doxorubicine, vincristine, prednisolone. Benda = bendamustine. DHAX = dexamethasone, cytarabine, oxaliplatin. GDP = Gemcitabine, dexamethasone, cisplatin. *This patient was one of the 5 patients who received R-Benda consolidation therapy following R-CHOP induction treatment.

Interestingly, group 3 that exhibits a differentiated and activated T-cell profile contained significantly more PR and progressor patients (5/8) than the two other groups characterized by T-cell profiles with low or intermediate activation markers (Fig. 4a) (Chi-squared test, $p = 0.015$). Moreover, before any treatment, PR and progressor patients exhibited significant lower frequencies of naive $CD4^+$ T cells, and decreased $CD4^+$ and $CD8^+$ T_N/T_{CM} ratios as compared to the others FL-patients and to healthy donors (Fig. 4b,c)

Rituximab-based therapy induces profound changes in peripheral T-cell subsets. We then examined changes occurring in the peripheral T-cell compartments during rituximab-based therapy (FL-T1 and FL-T2). The percentage of $CD4^+$ T_{CM} cells increased significantly at FL-T1 and FL-T2, whereas the percentages of T_N, T_{EM} and T_{reg} $CD4^+$ T cells decreased (Supplementary Fig. S5). For $CD8^+$ T-cell subsets, the percentage of T_N cells and T_{CM} increased while the percentages of T_{EM} and T_{EMRA} $CD8^+$ subsets decreased (Supplementary Fig. S5). Overall, these changes during treatment resulted in a decrease of the T_N/T_{CM} ratio and an increase of the T_{CM}/T_{EM} ratio in the $CD4^+$ T-cell compartment (Fig. 5a). T_N/T_{EM}, T_N/T_{EMRA}, T_{CM}/T_{EM}, and T_{CM}/T_{EMRA} ratios all increased in the $CD8^+$ T-cell compartment (Fig. 5b). Taken together, these results revealed a shift throughout treatment from a T_{EM} phenotype toward a T_{CM} phenotype for both $CD4^+$ and $CD8^+$ T-cell compartments and also toward a naive phenotype for $CD8^+$ T cells.

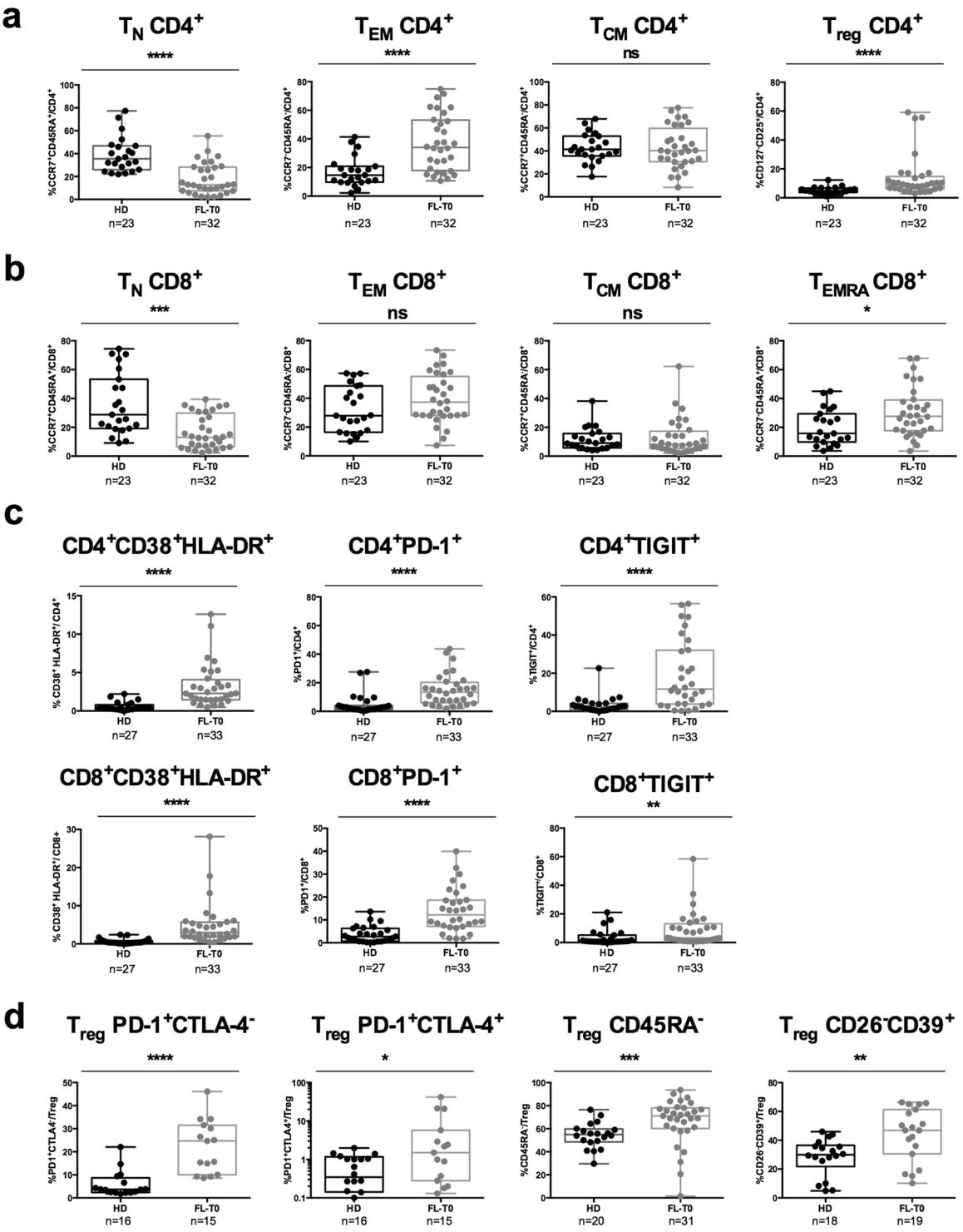

Figure 2. Analysis of peripheral T-cell subsets in FL patients before treatment. Box-and-whisker plots of flow cytometry data obtained from healthy donors (HD) and FL patients before treatment (FL-T0) blood samples. (**a**) Percentages of $CCR7^+CD45RA^+$ naive (T_N), $CCR7^-CD45RA^-$ (T_{EM}), $CCR7^+CD45RA^-$ (T_{CM}) and $CD127^-CD25^+$ (T_{reg}) $CD4^+$ T cells. (**b**) Percentages of T_N, T_{EM}, T_{CM} and $CCR7^-CD45RA^+$ (T_{EMRA}) $CD8^+$ T cells. (**c**) Percentages of $CD38^+HLA\text{-}DR^+$, $PD\text{-}1^+$ and $TIGIT^+$ among $CD4^+$ and $CD8^+$ T cells. (**d**) Percentages of $PD\text{-}1^+CTLA\text{-}4^-$, $PD\text{-}1^+CTLA\text{-}4^+$, $CD45RA^-$ and $CD26^-CD39^+$ among T_{reg}. The number of samples that have been successfully processed are indicated below each panel. A Mann-Whitney test was performed for statistical analyses. $^*p < 0.05$; $^{**}p < 0.01$; $^{***}p < 0.001$; $^{****}p < 0.0001$; ns: not significant.

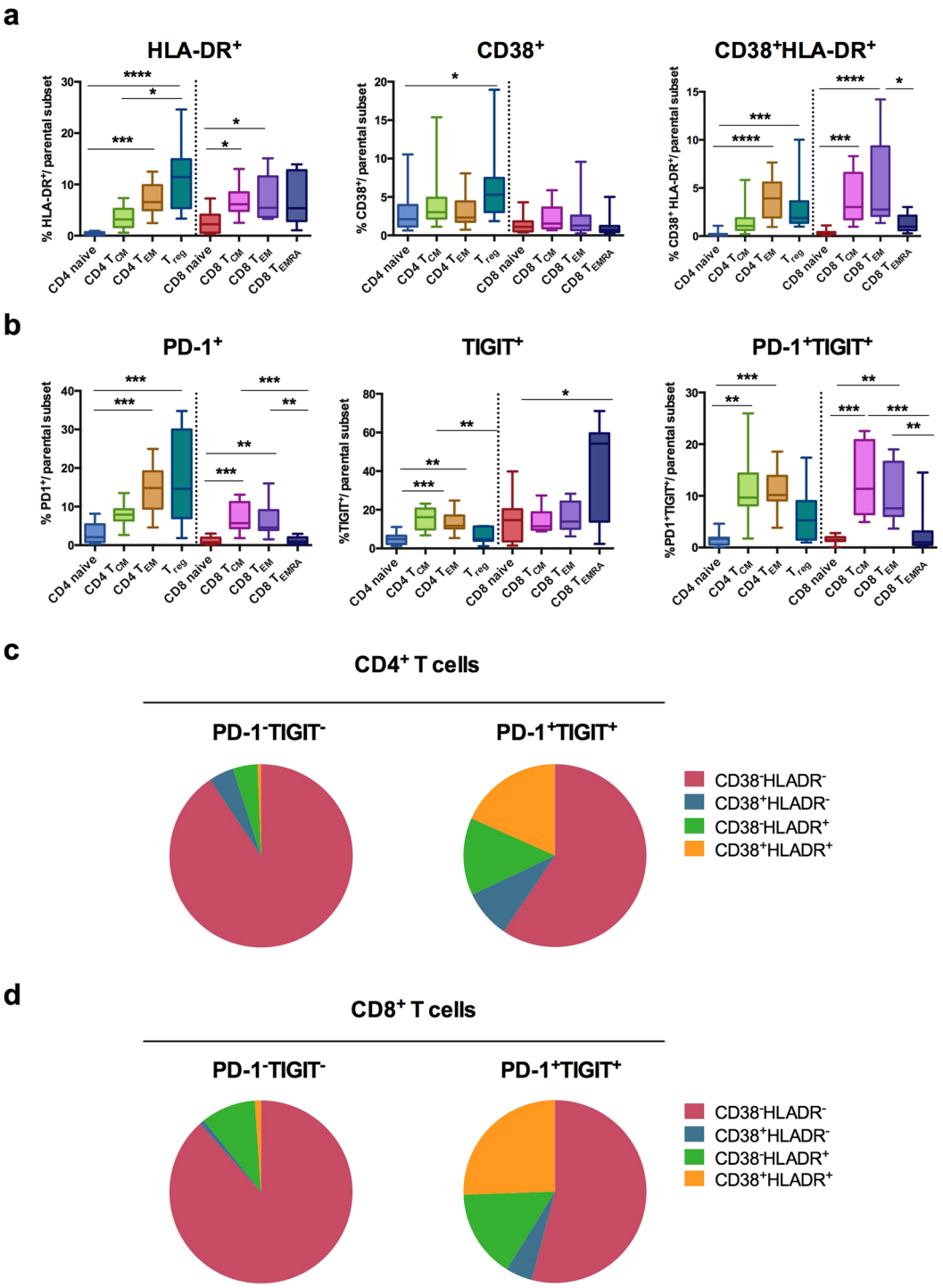

Figure 3. Activation status of peripheral T-cell subsets in FL patients before treatment. (**a**,**b**) Box-and-whisker plots of flow cytometry data obtained from blood samples of FL patients ($n = 11$) before treatment. Percentages of (**a**) HLA-DR$^+$, CD38$^+$, CD38$^+$HLA-DR$^+$ T cells and of (**b**) PD-1$^+$, TIGIT$^+$, and PD-1$^+$TIGIT$^+$ T cells among subsets of CD4$^+$ and CD8$^+$ T cells. (**c**,**d**) Pie chart of CD38/HLA-DR single-positive, double-positive and double-negative cells (slices represent the amount of each subset) among CD4$^+$ (**c**) or CD8$^+$ (**d**) T cells expressing PD-1 and TIGIT or not (indicated above each pie). A Kruskal-Wallis test followed by Dunn's multiple comparison test was performed for statistical analyses of flow cytometry data. *$p < 0.05$; **$p < 0.01$; ***$p < 0.001$; ****$p < 0.0001$.

The activation status of peripheral T cells changed during treatment. The percentages of peripheral CD4$^+$ T_{EM}, CD4$^+$$T_{CM}$ and CD8$^+$ T_{EM} cells expressing both HLA-DR and CD38, decreased during treatment (Fig. 5c). By contrast, the percentages of CD8$^+$ T_{CM} CD38$^+$HLA-DR$^+$ and CD8$^+$ T_{EMRA} CD38$^+$HLA-DR$^+$ remained stable during treatment (Fig. 5c).

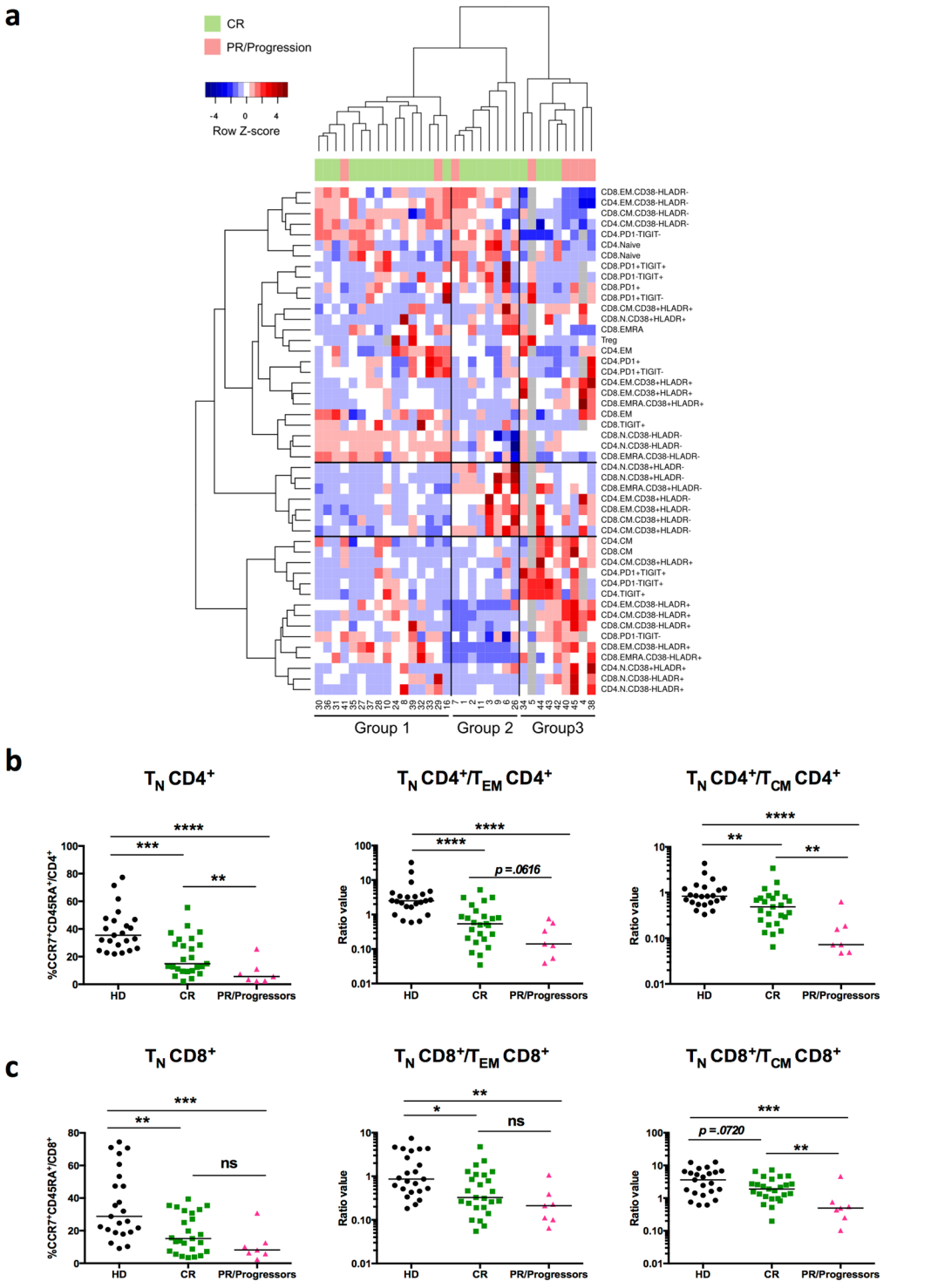

Figure 4. Heterogeneity of peripheral T-cell profiles in FL patients before treatment. (**a**) Hierarchical clustering of FL patients ($n = 33$) based on peripheral T-cell phenotypes before treatment. Phenotypes of analyzed T-cell subsets are indicated on the right. N indicates naive, CM central memory, EM effector memory, and EMRA effector memory RA^+, $CD4^+$ or $CD8^+$ T cells. Patient numbers are indicated below the diagram. The heatmap is colored according to row Z-scores. Some of the values are missing in three patients (grey squares). Patient response to treatment is indicated below column dendrogram. Green = complete responders (CR); pink = partial responders (PR) and progressors. **(b,c)** Scatter plots of flow cytometry data obtained from pre-treatment blood samples of CR patients ($n = 25$) or PR/progressors patients ($n = 7$) or healthy donors (HD, $n = 23$). (**b**) Percentages of $CCR7^+CD45RA^+$ naive (T_N) cells among $CD4^+$ T cells and ratios of $CD4^+$ T_N/T_{EM} or T_N/T_{CM} subsets. (**c**) Percentages of $CCR7^+CD45RA^+$ naive (T_N) among $CD8^+$ T cells and ratios of $CD8^+$ T_N/T_{EM} or T_N/T_{CM} subsets. A Mann-Whitney test was performed for statistical analyses. $^*p < 0.05$; $^{**}p < 0.01$; $^{***}p < 0.001$; $^{****}p < 0.0001$; ns: not significant.

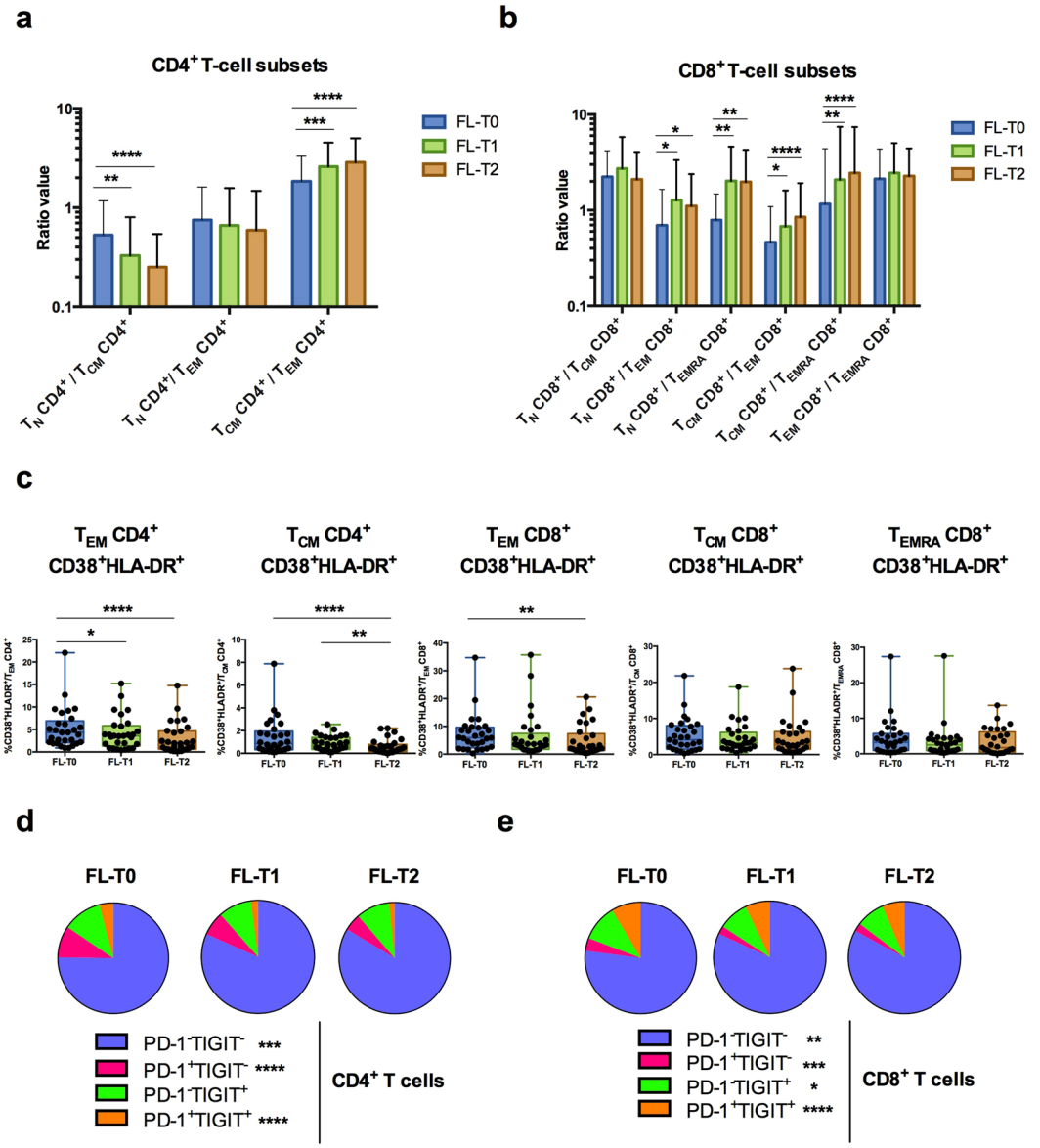

Figure 5. Changes in peripheral T-cell subsets in FL patients during therapy. Flow cytometry analysis of peripheral T-cell subsets in FL patients ($n = 29$) before (FL-T0) and during treatment (FL-T1; FL-T2). (**a**,**b**) Ratios of subsets of $CD4^+$ (**a**) and $CD8^+$ (**b**) T cells. (**c**) Box-and-whisker plots of percentages of $CD38^+$ $HLA\text{-}DR^+$ cells among T_{EM} and T_{CM} $CD4^+$ T cells and T_{EM}, T_{CM} and T_{EMRA} $CD8^+$ T cells. (**d**,**e**) Pie chart of PD-1/TIGIT single-positive, double-positive and double-negative cells among $CD4^+$ (**d**) or $CD8^+$ (**e**) T cells (slices represent amount of each subset). Friedman test followed by Dunn's multiple comparison test was performed for statistical analyses. $^*p < 0.05$; $^{**}p < 0.01$; $^{***}p < 0.001$; $^{****}P < 0.0001$; ns: not significant.

The percentages of $CD4^+$ and $CD8^+$ T cells expressing TIGIT and/or PD-1 decreased noticeably during rituximab-based therapy (Fig. 5d,e). This reduction was closely linked to a diminution of $PD\text{-}1^+TIGIT^-$ and $PD\text{-}1^+TIGIT^+$ subsets among $CD4^+$ T cells (Fig. 5d) and of $PD\text{-}1^+TIGIT^-$, $PD\text{-}1^-TIGIT^+$ and $PD\text{-}1^+TIGIT^+$ subsets for $CD8^+$ T cells (Fig. 5e), as well to a marked increase in the number of $PD\text{-}1^-TIGIT^-$ $CD4^+$ and $CD8^+$ cells (Fig. 5d,e). Unsupervised hierarchical clustering based on flow cytometry at FL-T1 and FL-T2 did not allow defining groups of patients for their response to treatment (data not shown).

Discussion

Studies using lymph node biopsies performed on retrospective cohorts of heterogeneous FL patient populations receiving various treatments have suggested that the amount of intra-tumor effector T cells expressing ICP, in particular TIM3, PD-1 and TIGIT, could have a prognostic value[22,23,34–36]. Only a few studies have investigated the phenotype of PBMC, in small-sized cohorts of untreated FL patients[20,21,23]. Modifications in the percentages of circulating naive helper $CD4^+$ T cells and T_{EMRA} $CD8^+$ T cells[21], and in the amount of blood T_{reg}[20], have been demonstrated. However, the evolution of the peripheral T-cell subsets during FL treatment and the relationship

between these subsets and the early response to R-CHOP have not yet been investigated. Thus, we have performed a longitudinal prospective study on peripheral blood from a small-sized cohort of similarly treated FL patients with high tumor burden, each receiving the same R-CHOP induction treatment followed by a maintenance treatment for most patients (25/33). Our study focused on the analysis of T-cell compartments, as preclinical data in mouse models as well as clinical investigations have suggested that T cells may play a major role in the control of tumor progression and in responses to antibody-based treatments[37].

Here, we show that at the time of the first treatment decision, FL patients with a high tumor burden exhibit low percentage of naive $CD4^+$ and $CD8^+$ T cells. Taken together, the decreased percentage of naive T cells associated with higher percentages of T_{EM} expressing both activation markers and ICP molecules and of terminally differentiated $TIGIT^+$ $CD8^+$ T_{EMRA} (Figs 2 and 3) reflects a strong activation of T cells during tumor development in FL patients before any treatment. However, the median age of FL patients may be higher than that of healthy donors. Thus, we cannot exclude that a number of differences in peripheral T-cell compartments (including fewer naive T cells and more T_{EMRA} $CD8^+$ T cells) observed in most untreated FL patients compared to healthy donors may be due, at least in part, to the senescence of the immune system, as previously observed for $CD8^+$ T cells in other studies[32,33]. Nonetheless, it should be noted that in our study, the age has no influence on the percentages of T_{reg} or of PD-1^+ and $TIGIT^+$ T cells in FL patients. Whether FL patients with low tumor burden also exhibit the same pattern of phenotypic changes remains to be investigated.

Interestingly, despite PD-1 and TIGIT expression on effector T cells, *in vitro* IFN-γ responses to CEFT-derived peptides were not modified in PBMC of FL patients as compared to healthy donors (Supplementary Fig. S3). These results are consistent with another study showing that inhibitory receptors expression (including PD-1, CTLA-4 and TIM-3) on peripheral T cells is associated with their differentiation and activation, and does not necessarily correlate with reduced functionality[38]. Moreover, in a recent study, Josefsson *et al*., showed that tumors from NHL patients were enriched in $CD4^+$ and $CD8^+$ T_{EM} cells expressing both PD-1 and TIGIT and exhibiting reduced effector functions in immunosuppressive tumor microenvironment, but normal cytokine production upon *in vitro* culture in absence of their ligands[39].

An unsupervised hierarchical clustering based on flow cytometry values led to the identification of three groups of patients with particular blood T-cell profiles (Fig. 4a). Group 3 exhibited a high frequency of T_{CM}, T_{EM}, and T_{EMRA} subsets expressing CD38 and/or HLA-DR activation markers, and high percentages of PD-1^+ and $TIGIT^+$ $CD4^+$ T cells. This group contained significantly more PR and progressor patients (5/8) than the two other groups (Fig. 4a). Previous reports have demonstrated an association between the expression of activation markers in FL lymph nodes with a rapid transformation to aggressive disease and a non-responsiveness to rituximab therapy[8,40]. Moreover, we found that PR and progressors patients exhibited a significant lower percentage of naive $CD4^+$ T cells, and decreased $CD4^+$ and $CD8^+$ T_N/T_{CM} ratios as compared to CR patients and healthy donors groups (Fig. 4b,c). Interestingly, a recent study using mass cytometry for analysis of $CD4^+$ T cell subsets in FL patient biopsies, has demonstrated that the frequency of intra-tumor naive T cells correlates with an improved patient survival[41]. These observations suggest that a careful investigation of T-cell profiles in the peripheral blood of FL patients with high tumor burden before treatment is of particular interest to decipher the mechanisms responsible for host failure to rituximab-based therapy.

Longitudinal flow cytometry phenotyping performed in FL patients also underlined changes in peripheral T-cell compartments during rituximab-based treatment. The therapy induced skewing of the T-cell compartment toward a $CD4^+$ T_{CM} and $CD8^+$ T_N/T_{CM} profile (Fig. 5). Although the different roles of T_{CM} and T_{EM} in immunity to infection are well described, many questions remain about which type of memory T cells are most beneficial for the development and maintenance of antitumor immunity. A comparison of the antitumor protection achieved by adoptively transferred tumor-reactive T_{CM} versus T_{EM} $CD8^+$ T cells revealed that the T_{CM} protective activity is superior to that of T_{EM}, primarily due to the T_{CM} lymphoid homing properties that increase their exposure to tumor-associated antigens presented by DCs[42]. Finally, a recent study showed that chimeric antigen receptor-modified T cells (CAR T cells) directed against CD19 molecule derived from either the T_N or T_{CM} subsets conferred a superior antitumor activity in a xenograft mouse model of B-cell lymphoma[43].

Part of the effects could be due to the CHOP (cyclophosphamide, vincristine, doxorubicin, prednisone) chemotherapy. It has been shown in humans or preclinical models that cyclophosphamide could deplete circulating T_{reg}, promote Th1, Th17 memory responses and CTL-dependent immune responses[44]. However, some studies in B-cell depleted mice and in rituximab-treated patients with autoimmune diseases suggest that the impact of R-CHOP on T-cell compartment is a direct consequence of B-cell depletion and the absence of T-cell/B-cell cooperation. Notably, it has been reported that B cell depletion after treatment with rituximab in autoimmune disorders affects T cell differentiation and activation, including down-regulation of costimulatory molecules and activation markers (eg, CD44, CD40L, CD69, HLA-DR, ICOS) on $CD4^+$ T cells, and increases in regulatory T cell numbers and suppressive functions[27]. Moreover, it has been shown that rituximab treatment could impact the naive/memory balance in T-cell subsets[45]. In naive mice treated with anti-mouse CD20 antibodies, short-term or chronic B-cell depletion disrupts $CD4^+$ and $CD8^+$ T cell homeostasis, in terms of naive, memory and effector T cell frequencies[26,46,47]. Also, immune responses to lymphocytic choriomeningitis virus (LCMV) infection are impaired, with a significant reduction in the number of IFN-γ and TNFα-producing T cells[46,47].

In our study, changes in peripheral T-cell profiles was accompanied by a decrease of the percentages of peripheral T cells expressing the ICP PD-1 and TIGIT. Moreover, the amount of peripheral $CD4^+$ T_{EM}, $CD4^+$ T_{CM} and $CD8^+$ T_{EM} cells expressing both HLA-DR and CD38 also decreased during treatment (Fig. 5). This suggests that the blood T-cell profile observed in high tumor burden FL patients could be at least partially reverted by rituximab-based treatment, and that anti-tumor activity could be reinforced by an increase in the number of $CD4^+$ T_{CM}, $CD8^+$ T_{CM} and $CD8^+$ T_N. Nevertheless, whether these changes have a long-term impact on the clinical outcome of high-tumor burden FL patients remains to be determined.

Methods

Ethical approval and ethical standards. This non-interventional study, which complies with the Declaration of Helsinki, was approved by the appropriate regional ethics committee ("Comités de Protection des Personnes", Ile-de-France, France) regulated by the government institution "Agence Régionale de Santé" (Bobigny, France), by the government advisory board for data processing in health care ("Comité Consultatif sur le Traitement de l'Information en matière de Recherche dans le Domaine de la Santé", Paris, France) (CCTIRS N°14.626), and by the French data protection authority ("Commission Nationale de l'Informatique et des Libertés", Paris, France) (CNIL N°DR-2015-237). All patients and healthy donors provided informed written consent to participate in this research study. For anonymous healthy donors, written informed consents were obtained by the French state agency EFS (www.efs.sante.fr).

Patients and study cohort. The 33 patients enrolled consecutively in the study from 2015 to 2016 were diagnosed with high tumor-burden FL and treated with a standard treatment regimen based on rituximab and chemotherapy (Hemato-oncology Department, Saint Louis hospital, Paris, France) (Table 1). High tumor-burden FL patients have at least one of the following features[3,48]: any nodal or extranodal tumor mass with a diameter of more than 7 cm; involvement of at least three nodal sites, each of which had a diameter of more than 3 cm; systemic symptoms; substantial splenic enlargement; serous effusion, orbital or epidural involvement, or ureteral compression (alone or in combination); and leukemia. All patients received an induction therapy (R-CHOP) consisting of six cycles every 21 days of rituximab combined to chemotherapy (cyclophosphamide, doxorubicine, vincristine, prednisolone). R-CHOP responder patients then received rituximab maintenance for two years. Flow chart of patient treatment is detailed in Fig. 1. Blood samples were collected before treatment (FL-T0) and at two different time points during treatment (FL-T1 at three months and FL-T2 at 8–12 months after initiation of treatment) as described in Supplementary Table S1. Blood samples from anonymized healthy donors (HD) were obtained from the French blood agency (EFS). Peripheral blood mononuclear cells (PBMC) were obtained from heparinized blood tubes by Hypaque-Ficoll centrifugation. HLA-A, -B, -C, -DRB1, -DQB1 and -DPB1-typing of patients were performed using the PCR-SSO (Polymerase Chain Reaction-Sequence Specific Oligoprobe) molecular method using the LABType SSO kits from One Lambda Inc. (Canoga).

Flow cytometry. Cryopreserved PBMC samples from each patient from the different time points were tested in the same experiment, along with control samples from healthy donors. PBMC were stained with antibodies mixed in panels described in Supplementary Table S2. Data were acquired with a LSR Fortessa flow cytometer (BD Biosciences) and analyzed with Kaluza software (version 1.3, Beckman Coulter). Two different antibody panels were used to enable discrimination of $CD3^+$ conventional T-cell subsets (Panel 1, Supplementary Table S2), including $CD4^+$ and $CD8^+$ T cells, $CD45RA^+CCR7^+$ naive T cells (T_N), $CD45RA^-CCR7^+$ central memory T cells (T_{CM}), $CD45RA^-CCR7^-$ effector memory T cells (T_{EM}), $CD45RA^+CCR7^-$ effector memory RA cells (T_{EMRA}), and of $CD4^+$ $CD127^-CD25^+$ regulatory T cells (T_{reg}) (Panel 2, Supplementary Table S2). The expression of CD27 and CD28 was also evaluated to confirm the phenotype of the different T-cell subsets[32,49]. A third panel also made it possible to evaluate the expression of different activating and inhibitory ICP (OX40, CD40L, GITR, 4-1BB, LAG3, TIM3, TIGIT, PD-1) to determine the activation status of peripheral $CD4^+$ and $CD8^+$ T cells (Panel 3, Supplementary Table S2). A fourth panel enables analysis of the co-expression of CD38 and HLA-DR, PD-1 and TIGIT on the different T-cell subsets (Panel 4, Supplementary Table S2).

IFN-γ ELISPOT assays. $1–2 \times 10^5$ PBMC/well were incubated in IFN-γ ELISPOT plates (CTL) for 36 hours in serum-free medium with a single mixture of MHC-I and MHC-II restricted peptides derived from cytomegalovirus (CMV), Epstein-Barr virus (EBV), Influenza virus and tetanus toxin (CEFT peptides, 4 μg/mL each) (Panatecs). A positive threshold was set at $\geq$10 spot-forming-units (SFU) per 10^5 cells after subtracting the background noise as previously described[50]. Each sample was tested in triplicate and the mean value was reported.

Statistical analyses. Statistical evaluation of the results for flow cytometry and ELISPOT assays were performed using nonparametric unpaired (Kruskal-Wallis, Mann-Whitney), nonparametric paired (Friedman), and Spearman correlation tests (indicated in each figure legend). Kruskal-Wallis and Friedman tests were followed by *post-hoc* tests (Dunn's multiple comparison test), performed with Prism software (version 5, Graphpad, San Diego, CA, USA). In one experiment, unpaired *t* tests with Bonferroni correction for multiple testing were used. Unsupervised hierarchical clustering was performed using R software (version 3.3.1), with Euclidian distance and Ward linkage criterion. A Chi-square test was used for comparison of the number of complete responders (CR) and partial responders (PR) patients among the groups defined by hierarchical clustering. *p* values for all statistical tests performed were considered significant when <0.05.

Data Availability

The datasets generated during and/or analysed during the current study are available from the corresponding author on reasonable request (sophie.siberil@sorbonne-universite.fr).

References

1. Freedman, A. Follicular lymphoma: 2018 update on diagnosis and management. *Am. J. Hematol.* **93**, 296–305 (2018).
2. Hiddemann, W. *et al.* Frontline therapy with rituximab added to the combination of cyclophosphamide, doxorubicin, vincristine, and prednisone (CHOP) significantly improves the outcome for patients with advanced-stage follicular lymphoma compared with therapy with CHOP alone: results of a prospective randomized study of the German Low-Grade Lymphoma Study Group. *Blood.* **106**, 3725–3732 (2005).
3. Salles, G. *et al.* Rituximab maintenance for 2 years in patients with high tumour burden follicular lymphoma responding to rituximab plus chemotherapy (PRIMA): a phase 3, randomised controlled trial. *Lancet.* **377**, 42–51 (2011).

4. Casulo, C. *et al*. Early relapse of follicular lymphoma after rituximab plus cyclophosphamide, doxorubicin, vincristine, and prednisone defines patients at high risk for death: an analysis from the National LymphoCare Study. *J. Clin. Oncol.* **33**, 2516–2522 (2015).
5. Jurinovic, V. *et al*. Clinicogenetic risk models predict early progression of follicular lymphoma after first-line immunochemotherapy. *Blood.* **128**, 1112–1120 (2016).
6. Huet, S. *et al*. A gene-expression profiling score for prediction of outcome in patients with follicular lymphoma: a retrospective training and validation analysis in three international cohorts. *Lancet Oncol.* **19**, 549–561 (2018).
7. Dave, S. S. *et al*. Prediction of survival in follicular lymphoma based on molecular features of tumor-infiltrating immune cells. *N. Engl. J. Med.* **351**, 2159–2169 (2004).
8. Glas, A. M. *et al*. Gene-expression and immunohistochemical study of specific T-cell subsets and accessory cell types in the transformation and prognosis of follicular lymphoma. *J. Clin. Oncol.* **25**, 390–398 (2007).
9. Byers, R. J. *et al*. Clinical quantitation of immune signature in follicular lymphoma by RT-PCR-based gene expression profiling. *Blood.* **111**, 4764–4770 (2008).
10. Alvaro, T. *et al*. Immunohistochemical patterns of reactive microenvironment are associated with clinicobiologic behavior in follicular lymphoma patients. *J. Clin. Oncol.* **24**, 5350–5357 (2006).
11. Wahlin, B. E., Sander, B., Christensson, B. & Kimby, E. CD8+ T-cell content in diagnostic lymph nodes measured by flow cytometry is a predictor of survival in follicular lymphoma. *Clin. Cancer Res.* **13**, 388–397 (2007).
12. Carreras, J. *et al*. High numbers of tumor-infiltrating programmed cell death 1-positive regulatory lymphocytes are associated with improved overall survival in follicular lymphoma. *J. Clin. Oncol.* **27**, 1470–1476 (2009).
13. Gribben, J. G. Implications of the tumor microenvironment on survival and disease response in follicular lymphoma. *Curr. Opin. Oncol.* **22**, 424–430 (2010).
14. Wahlin, B. E. *et al*. A unifying microenvironment model in follicular lymphoma: outcome is predicted by programmed death-1–positive, regulatory, cytotoxic, and helper T cells and macrophages. *Clin. Cancer Res.* **16**, 637–650 (2010).
15. Wahlin, B. E. *et al*. T cells in tumors and blood predict outcome in follicular lymphoma treated with rituximab. *Clin. Cancer Res.* **17**, 4136–4144 (2011).
16. de Jong, D. & Fest, T. The microenvironment in follicular lymphoma. *Best Pract. Res. Clin. Haematol.* **24**, 135–146 (2011).
17. Yang, Z. Z. & Ansell, S. M. The tumor microenvironment in follicular lymphoma. *Clin. Adv. Hematol. Oncol.* **10**, 810–818 (2012).
18. Amé-Thomas, P. & Tarte, K. The yin and the yang of follicular lymphoma cell niches: role of microenvironment heterogeneity and plasticity. *Semin. Cancer Biol.* **24**, 23–32 (2014).
19. Blaker, Y. N. *et al*. The tumour microenvironment influences survival and time to transformation in follicular lymphoma in the rituximab era. *Br. J. Haematol.* **175**, 102–114 (2016).
20. Mittal, S. *et al*. Local and systemic induction of CD4+CD25+ regulatory T-cell population by non-Hodgkin lymphoma. *Blood.* **111**, 5359–5370 (2008).
21. Christopoulos, P. *et al*. Definition and characterization of the systemic T-cell dysregulation in untreated indolent B-cell lymphoma and very early CLL. *Blood.* **117**, 3836–3846 (2011).
22. Yang, Z. Z. *et al*. IL-12 upregulates TIM-3 expression and induces T cell exhaustion in patients with follicular B cell non-Hodgkin lymphoma. *J. Clin. Invest.* **122**, 1271–1282 (2012).
23. Myklebust, J. H. *et al*. High PD-1 expression and suppressed cytokine signaling distinguish T cells infiltrating follicular lymphoma tumors from peripheral T cells. *Blood.* **121**, 1367–1376 (2013).
24. de Jong, D. *et al*. Impact of the tumor microenvironment on prognosis in follicular lymphoma is dependent on specific treatment protocols. *Haematologica.* **94**, 70–77 (2009).
25. Xerri, L. *et al*. Rituximab treatment circumvents the prognostic impact of tumor-infiltrating T-cells in follicular lymphoma patients. *Hum. Pathol.* **64**, 128–136 (2017).
26. Lund, F. E. & Randall, T. D. Effector and regulatory B cells: modulators of CD4+ T cell immunity. *Nat. Rev. Immunol.* **10**, 236–247 (2010).
27. Kessel, A., Rosner, I. & Toubi, E. Rituximab: beyond simple B cell depletion. *Clin. Rev. Allergy Immunol.* **34**, 74–79 (2008).
28. Abès, R., Gélizé, E., Fridman, W. H. & Teillaud, J. L. Long-lasting antitumor protection by anti-CD20 antibody through cellular immune response. *Blood.* **116**, 926–934 (2010).
29. Deligne, C., Metidji, A., Fridman, W. H. & Teillaud, J. L. Anti-CD20 therapy induces a memory Th1 response through the IFN-γ/IL-12 axis and prevents protumor regulatory T-cell expansion in mice. *Leukemia.* **29**, 947–957 (2015).
30. DiLillo, D. J. & Ravetch, J. V. Differential Fc-Receptor Engagement Drives an Anti-Tumor Vaccinal Effect. *Cell.* **161**, 1035–1045 (2015).
31. Ren, Z. *et al*. CTLA-4 Limits Anti-CD20-Mediated Tumor Regression. *Clin. Cancer Res.* **23**, 193–203 (2017).
32. Koch, S. *et al*. Multiparameter flow cytometric analysis of CD4 and CD8 T cell subsets in young and old people. *Immun. Ageing.* **5**, 6, https://doi.org/10.1186/1742-4933-5-6 (2008).
33. Saavedra, D., Garcia, B. & Lage, A. T cell subpopulations in healthy elderly and lung cancer patients: Insights from Cuban Studies. *Front. Immunol.* **8**, 146, https://doi.org/10.3389/fimmu.2017.00146 (2017).
34. Yang, Z. Z. *et al*. TGF-β upregulates CD70 expression and induces exhaustion of effector memory T cells in B-cell non-Hodgkin's lymphoma. *Leukemia.* **28**, 1872–1884 (2014).
35. Josefsson, S. E. *et al*. T cells expressing checkpoint receptor TIGIT are enriched in Follicular Lymphoma tumors and characterized by reversible suppression of T-cell receptor signaling. *Clin. Cancer Res.* **24**, 870–881 (2018).
36. Yang, Z. Z. *et al*. PD-1 expression defines two distinct T-cell sub-populations in follicular lymphoma that differentially impact patient survival. *Blood Cancer J.* **5**, e281, https://doi.org/10.1038/bcj.2015.1 (2015).
37. Deligne, C., Milcent, B., Josseaume, N., Teillaud, J. L. & Sibéril, S. Impact of depleting therapeutic monoclonal antibodies on the host adaptive immunity: a bonus or a malus? *Front. Immunol.* **8**, 950, https://doi.org/10.3389/fimmu.2017.00950 (2017).
38. Legat, A., Speiser, D. E., Pircher, H., Zehn, D. & Fuertes Marraco, S. A. Inhibitory Receptor Expression Depends More Dominantly on Differentiation and Activation than "Exhaustion" of Human CD8 T Cells. *Front. Immunol.* **4**, 455, https://doi.org/10.3389/fimmu.2013.00455 (2013).
39. Josefsson, S. E. *et al*. TIGIT and PD-1 Mark Intratumoral T Cells with Reduced Effector Function in B-cell Non-Hodgkin Lymphoma. *Cancer Immunol. Res.* **7**, 355–362 (2019).
40. Bohen, S. P. *et al*. Variation in gene expression patterns in follicular lymphoma and the response to rituximab. *Proc. Natl. Acad. Sci. USA* **100**, 1926–1930 (2003).
41. Yang, Z. Z. *et al*. Mass Cytometry Analysis Reveals that Specific Intratumoral CD4+ T Cell Subsets Correlate with Patient Survival in Follicular Lymphoma. *Cell Rep.* **26**, 2178–2193 (2019).
42. Klebanoff, C. A. *et al*. Central memory self/tumor-reactive CD8+ T cells confer superior antitumor immunity compared with effector memory T cells. *Proc. Natl. Acad. Sci. USA* **102**, 9571–9576 (2005).
43. Sommermeyer, D. *et al*. Chimeric antigen receptor-modified T cells derived from defined CD8+ and CD4+ subsets confer superior antitumor reactivity *in vivo*. *Leukemia.* **30**, 492–500 (2016).
44. Galluzzi, L., Buqué, A., Kepp, O., Zitvogel, L. & Kroemer, G. Immunological Effects of Conventional Chemotherapy and Targeted Anticancer Agents. *Cancer Cell.* **28**, 690–714 (2015).

45. Sentís, A. *et al*. Kinetic analysis of changes in T- and B-lymphocytes after anti-CD20 treatment in renal pathology. *Immunobiology.* **222**, 620–630 (2017).
46. Lykken, J. M. *et al*. Acute and chronic B cell depletion disrupts CD4+ and CD8+ T cell homeostasis and expansion during acute viral infection in mice. *J. Immunol.* **193**, 746–756 (2014).
47. Misumi, I. & Whitmire, J. K. B cell depletion curtails CD4+ T cell memory and reduces protection against disseminating virus infection. *J. Immunol.* **192**, 1597–1608 (2014).
48. Solal-Celigny, P. *et al*. Recombinant interferon alfa-2b combined with a regimen containing doxorubicin in patients with advanced follicular lymphoma. Groupe d'Etude des Lymphomes de l'Adulte. *N. Engl. J. Med.* **329**, 1608–1614 (1993).
49. Hamann, D. *et al*. Phenotypic and functional separation of memory and effector human CD8+ T cells. *J. Exp. Med.* **186**, 1407–1418 (1997).
50. Godet, Y. *et al*. Analysis of spontaneous tumor-specific CD4 T-cell immunity in lung cancer using promiscuous HLA-DR telomerase-derived epitopes: potential synergistic effect with chemotherapy response. *Clin. Cancer Res.* **18**, 2943–2953 (2012).
51. Solal-Céligny, P. *et al*. Follicular lymphoma international prognostic index. *Blood.* **104**, 1258–1265 (2004).

Acknowledgements

The authors thank Patricia Rezgui (Hemato-oncology Department, Saint Louis hospital, Paris, France) for blood sample collection and all the patients who contributed to this study. English writing assistance was provided by Jo Ann Cahn. Benoit Milcent was supported by a fellowship from CARPEM (Cancer Research for Personalized Medicine) association. Sophie Sibéril was supported by a grant from Fondation ARC pour la recherche sur le cancer (Grant number, ARC PJA20131200475) and Jean-Luc Teillaud and Sophie Sibéril by funding from INSERM, Sorbonne University and Paris-Descartes University. Catherine Thieblemont is funded by the Nella and Amadeus Barletta foundation (FNAB).

Author Contributions

B.M., P.B., C.T., J.-L.T. and S.S. designed the study. S.A., P.B. and C.T. provided cases for the study. B.M., Q.R., N.J. and S.S. performed and analyzed the experiments. J.-L.T. analyzed the experiments. F.P. helped to analyze data. P.L. and A.T. performed HLA-typing. B.M., S.S. and J.-L.T. wrote the manuscript. All authors critically reviewed the manuscript and approved the final version.

Additional Information

Supplementary information accompanies this paper at https://doi.org/10.1038/s41598-019-50029-y.

Competing Interests: The authors declare no competing interests.

Publisher's note Springer Nature remains neutral with regard to jurisdictional claims in published maps and institutional affiliations.